A Sensitivity Study of Wave and Wind Induced Responses of the Combined Energy Concept SFC Based on Experimental Measurements

Constantine Michailides, Zhen Gao and Torgeir Moan
Centre for Ships and Ocean Structures (CeSOS), Centre for Autonomous Marine Operations and Systems (AMOS), Department of Marine Technology, Norwegian University of Science and Technology (NTNU)
Trondheim, Norway

ABSTRACT

This paper deals with a sensitivity study of the combined energy concept SFC in operational and survival conditions. The sensitivity study is conducted based on experimental data. The measured responses that are studied include motions of the semisubmersible, rotation of the flap-type WECs, tension of mooring lines, internal loads of the arms of the WECs, bending moment at the base of wind turbines tower and produced power by WECs. The effect of the change of the mean heeling angle of the SFC and of the aerodynamic damping is studied. The effect of the wind loading in structural responses of different parts of WECs is small.

KEY WORDS: Semisubmersible Flap Combination (SFC); Offshore combined energy concepts; Physical model testing; Survivability; Functionality.

INTRODUCTION

Offshore renewable energy systems are expected to significantly contribute in the coming years to reach the energy security targets worldwide. The technology in offshore renewable energy sector that can be considered mature enough is the Offshore Wind Turbines (OWTs) technology. The Levelised Cost Of Energy (LCOE) of OWTs in the 2013 is in the range of 130-330 USD/MWh (World Energy Council, 2013). The cost of OWTs is the main handicap for their further utilization. In order to reduce the cost of generated power, the development of large rated wind turbines in deep sea is considered as an efficient potential direction for offshore wind energy. For deep waters the use of Floating type OWTs (FOWTs) is considered as the most efficient. Different floating support platform configurations are possible for use with FOWTs (Jonkman and Matha, 2011). A major type of support configuration is the semisubmersible platform consisting of columns that are connected with the use of braces (Robertson et al., 2014; Roddier et. al, 2010). Alternatively, the columns of the semisubmersible platform can be connected by pontoons with large dimensions without braces (Olav Olsen, 2013; Luan et al., 2015; Karimirad and Michailides, 2015).

Ocean waves are an extremely abundant and promising resource of alternative and clean energy. Many different types of Wave Energy Converters (WECs) have been proposed. The first patent of a WEC has been registered in 1799 in France by a father and a son named Girard (Michailides, 2015). Unfortunately the technology of WECs cannot be considered yet as mature for large-scale commercial deployment. The LCOE of WECs in the 2013 is in the range of 280-1000 USD/MWh (World Energy Council, 2013).

It might be beneficial to combine offshore renewable energy systems of different technology into one floating platform. Recently, EU research projects have been introduced to accelerate the development of combined offshore energy systems; these projects are the MARINA Platform (2015), ORECCA (2015), TROPOS (2015), H2Ocean (2015) and MERMAID (2015). Possible advantages as a result of the use of offshore combined concepts are: (a) increase of the energy production per unit area of space, (b) decrease of the cost related to the support platform, (c) decrease of the cost related with the required electric grid infrastructure and (d) decrease of the costs related to operation (e.g. installation) and maintenance (e.g. inspection).

In the EU project MARINA Platform three combined concepts have been selected and studied both numerically and experimentally. These three combined concepts are the Semisubmersible Flap Combination (SFC) (Michailides et al., 2014) the Spar Torus Combination (STC) (Muliawan et al., 2013) and an array of oscillating water columns (OWC) in a V-shaped concrete large floating platform and one wind turbine combination (O'Sullivan and Murphy, 2013). The combined concept SFC consists of a braceless semisubmersible floating platform, a 5 MW wind turbine, three rotating flap-type WECs and three catenary mooring lines (Fig. 1).

As far as physical model testing of OWTs is concerned, there are different techniques for the physical modeling of the rotor, tower and thrust force. Also, one important uncertainty related to interpretation of the model test results is the scaling effect (e.g. Müller et al., 2014). The rotor can be simplified as a disk providing a drag force (Roddier et al., 2010) or as a controlled fan providing an active force (Azcona et al., 2014; Huijs et al., 2014). A geometrically scaled rotor according to Froude's law will produce less corresponding thrust force at model

scale as compared to a full scale rotor (Fowler et al., 2013) and a redesign of the rotor blade is necessary to achieve the correct scaled thrust curve (Martin et al., 2012). Moreover, the external radius of the tower should be as small as possible since higher wind speeds are used for the selected redesigned rotor and the corresponding wind loading on the tower will be higher in the basin compared to the full scale one.

Figure 1. Artistic 3D bird view of the SFC

In the testing of a fixed bottom rotating flap-type WEC, Flocard and Finnigan (2010) modelled the PTO with an adjustable rotary viscous dashpot that is connected with a rotation shaft that is out of the water. Alternatively Ogai et al. (2010) modelled the PTO of the rotating flap with a gear transmission system and a piston-type air compressor. For the case of a floating bottom rotating flap-type WEC, Pecher et al. (2010) modelled the PTO with the use of a load adaptable friction wagon mounted on a rail, a potentiometer and a force transducer.

So far experimental investigations of combined wind/wave concepts have been reported by Gao et al. (2015), Wan et al. (2015) and Wan et al. (2016) based on different physical model set-up strategies of different parts of the combined concepts. Michailides et al. (2016a, 2016b) compared the experimental responses of the SFC in operational and extreme conditions with numerical predictions. Numerical studies of the response of the SFC are reported by Michailides et al. (2014; 2015) and Luan et al. (2014).

The present paper deals with a sensitivity study of the SFC based on experiments. The comparison is conducted for two different experimental campaigns of the SFC. The first corresponds to the survivability physical model of the SFC in which the wind turbine is parked and the WECs are released to freely rotate; the SFC is not producing power. The second corresponds to the functionality physical model of SFC where the blades of the wind turbine rotate and the PTOs of WECs are in operation behaving as linear dampers; the SFC is in operation and produces power. Regular and irregular wave and wind tests are conducted subjected to aligned wind and wave conditions. First the physical model test set-up of the 1:50 scale model of the SFC is described. Two possible effects of wind loading on the hydrodynamic loads and wave-induced responses are investigated; the change of the mean heeling angle of the SFC due to the mean thrust force of the rotor and the aerodynamic damping that may have a significant effect on the slowly-varying motions of the SFC induced by the second-order wave loads for irregular waves. The quantification of these effects, by comparing the responses under wave loads and under wind and wave loads, is discussed. The measured responses that are compared include motions of the semisubmersible platform in six rigid body degrees of freedom, rotation of the flap-type WECs, tension of mooring lines, internal loads of the arms that connect the rotating flaps with the pontoon of the semisubmersible platform, bending moment at the base of the turbines tower and produced power by WECs. The results obtained demonstrate the dominance of wave loading in some responses mainly with regard to the response of WECs.

DESCRIPTION OF THE PHYSICAL MODEL SET-UP

The survivability and functionality tests of the SFC have been conducted in the Hydrodynamics and Ocean Engineering Tank in Ecole Centrale Nantes (ECN), France. In ECN's basin the wave and wind loadings can be generated by two different generation systems. Regular and irregular directional waves are generated by a multiflap wavemaker system with 48 independent flaps. Moreover, a wind generation system capable for generating wind speed up to 10 m/sec in model scale is used. The wind generation system (Courbois et al., 2013) is composed by eight centrifugal fans placed on the side of the basin and produces airflow via flexible air ducts to the centre of the basin and close to the physical model of SFC. A sketch of the plan view of the basin as well as of the arrangement of SFC during the tests is presented in Figure 2. The survivability and functionality physical models of SFC are presented in Fig. 3a and Fig. 3b, respectively. The basic difference between the two physical models is that the PTO configuration of the three WECs is not in operation and the WECs are released to freely rotate in the survivability model. For the functionality model The damping coefficients isof WEC's PTOs is equal to 1,230 kNms/deg, 528 214 kNms/deg, 528 kNms/deg for WEC1, WEC2 and WEC3, respectively. Also, the wind turbine is parked in the survivability model while in the functionality model the blades of the wind turbine rotate around their axis of rotation. Finally, the draft of the platform is 31.25m and 30.0m for the survivability and functionality model, respectively.

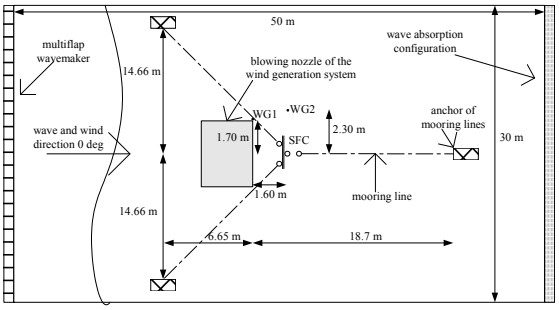

Figure 2. Plan view of the experimental set-up of SFC at ECN

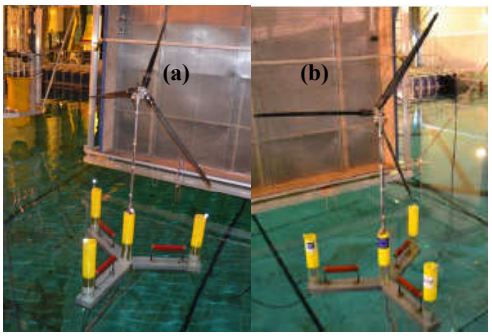

Figure 3. Survivability (Fig. 3a) and functionality (Fig. 3b) physical model of SFC at ECN

Froude laws of similitude have been used for the physical modelling of the properties of the semisubmersible platform and rotating flap-type WECs (Table 1). Each WEC consists of one fully submerged flap with elliptical shape, two cylindrical shaped arms and one rotating shaft (axis of rotation). The rotating flap has been built by synthetic foam, while the arms and the shaft are made of titanium material. The upper point of the flap in its mean position is 2 m and 3.25 m below the Mean Water Level (MWL) for the functionality and survivability model, respectively, and the lower point of the flap is 15 m above the pontoon

of the semi-submersible platform for both physical models. Each arm is rigidly connected with the flap at the higher ends as well as is connected at the lower ends with a shaft that is mounted to the pontoon of the semisubmersible platform in two low friction bearings. Additionally, the shaft through a third low bearing is inserted into the adjacent side column of the semisubmersible platform and connected with a PTO configuration, which is used to physically model the linear PTO of the WEC. The PTO configuration consists of a lower and an upper pulley, a timing belt, two tensioners and a linear mechanical rotary damper. The damping coefficient of the mechanical rotary damper, C_{PTO}, was manually adjusted to have a constant value prior to the tests. The instantaneous WEC's produced power is:

$$P(t) = C_{PTO}\dot{\theta}(t)^2 \quad \text{(Eq. 1)}$$

where $\dot{\theta}(t)$ is the velocity of the rotation of the shaft.

As far as the modelling of the wind turbine, a redesigned small-scale rotor has been used in model scale as compared to the NREL 5 MW reference wind turbine (Jonkman et al. 2009). Since the same Reynolds number cannot be achieved in the physical model, the blades of the wind turbine were redesigned in order to produce the correct thrust force relative to Froude laws of similitude. In Table 2 structural properties of different parts of the wind turbine that were used for the survivability and functionality tests of SFC are presented. More details with regard to the design of the wind turbine as well as to the generated thrust force are presented in Courbois (2013).

Table 1. Scaling factors that were used for different variables

Variables	Scale factor	
Linear dimensions (length, height, width, wave height etc)	λ	50
Mass, Force	λ^3	125,000
Time, Velocity	$\lambda^{0.5}$	7.07
Moment	λ^4	6,250,000
Produced power by WECs	$\lambda^{3.5}$	883,883.5

Table 2. Structural properties of different parts of wind turbine

Variables	SFC
Blade length [m]	61.15
Blade mass [kg]	16,875
Blade Flapwise flexible mode [Hz]	1.032
Nacelle mass [kg]	243,750
Shaft tilt [°]	5
Hub mass [kg]	79,375
Vertical distance of hub to the MWL [m]	90
Horizontal distance of hub to the tower [m]	4.98
Tower mass [kg]	226,250
Diameter of tower [m]	1.1
Tower's first bending mode [Hz]	0.605

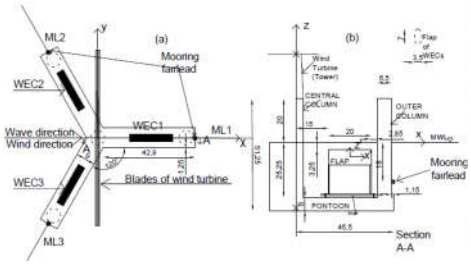

Figure 4. Plane view (Fig. 4a) and side view (Fig. 4b) of SFC

In Fig. 4 main dimensions of different parts of the survivability model of SFC in full scale are presented. In Table 3 properties of the main components of the SFC are presented in full scale values. In Fig. 5 different parts and sensors of the physical model of SFC that were used are presented. The sampling rate of all the sensors that were used during the experiments is equal to 120 Hz.

Table 3. Structural properties of main components of SFC

Variables	SFC
COG of the whole SFC (x,y,z) [m]	(0,0,-0.367)
I_{xx} (kg*m^2) of the platform	11,445,542,000
I_{yy} (kg*m^2) of the platform	11,445,542,000
I_{zz} (kg*m^2) of the platform	9,772,627,000
Mass of each flap [kg]	100,000
Displacement of each flap [kg]	395,000
WEC $I_{x'x'}$ local coordinate system (kg*m^2)	656,250
WEC $I_{y'y'}$ (kg*m^2)	4,496,875
WEC $I_{z'z'}$ (kg*m^2)	4,168,750

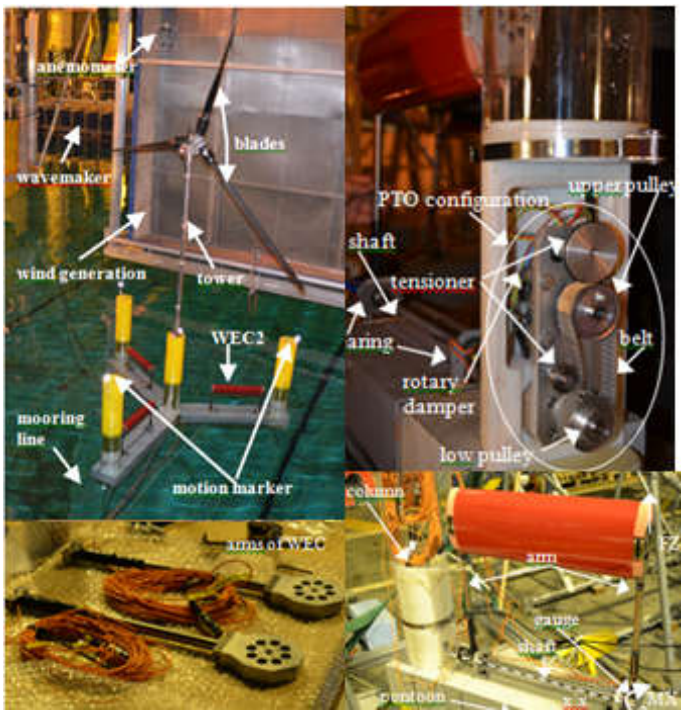

Figure 5. Survivability model of SFC placed into the basin (Fig. 5a), PTO configuration of functionality model of SFC (Fig. 5b), arms of WECs (Fig. 5c) ans WEC2 configuration (Fig. 5d).

As far as the generated environmental conditions, two wave gauges (WG1 and WG2) have been used for measuring the water free surface elevation and a wind load cell (sonic anemometer) has been used for measuring the wind velocity. The wind thrust force has been measured with the use of a force sensor that measures the shear force response (positive X direction) on the tower top.

As far as the mooring lines, three catenary mooring lines made by inox chain are used with weight in air per unit length equal to 152.5 kg/m.

Based on experimental decay tests in Table 5 the natural periods of surge, heave and pitch motion of the semisubmersible platform and rotation of WEC2 of the survivability model, $T_{exp,surv}$, and of the functionality model, $T_{exp,fun}$, are presented.

Table 5. Natural periods of surge, heave and pitch motion of the semisubmersible platform and rotation of WEC2

Degree of freedom	$T_{exp,surv}$ (sec)	$T_{exp,fun}$ (sec)
Surge	114.76	113.066
Heave	26.445	26.233
Pitch	34.789	34.548
WEC_2 rotation	14.778	14.483

COMPARISONS OBTAINED WITH THE SFC SURVIBALITY MODEL

The environmental conditions, for which comparisons of the wave-induced responses with wave-wind-induced responses based on experiments of the survivability model of SFC are conducted, are presented in Table 6. The conditions correspond to irregular waves without or with wind loadings. For the survivability model regular wave tests have been conducted only with wind loading and are not presented in the present paper. EEC1 ~ EEC4 correspond to tests with wave only loadings while EEC1W ~ EEC4W correspond to tests with wave and wind loadings. As far as the tests with wave and wind loading EEC1W ~ EEC4W, the turbulence intensity of the measured wind data are 0.102, 0.108, 0.101 and 0.092 for EEC1W, EEC2W, EEC3W and EEC4W, respectively. In Figure 6 comparison of spectra of wave elevation in WG1 for extreme environmental conditions is presented. As far as the extreme environmental conditions that are concerned, the Site no. 14 and Site no. 3 of the MARINA platform project was selected (Li et al., 2015) and two different conditions (condition with maximum wind speed, Uw, or with maximum significant wave height, Hs) for each site considering the 50 year maximum return values have been considered.

Table 6. Examined extreme environmental conditions in full scale values

Extreme conditions	Hs (m)	Tp (sec)	Uw (m/sec)
EEC1	8.8	14.8	-
EEC2	13.5	15	-
EEC3	11.5	15.7	-
EEC4	15.3	15.5	-
EEC1W	8.8	14.8	27.9
EEC2W	13.5	15	33.3
EEC3W	11.5	15.7	24.3
EEC4W	15.3	15.5	31.4

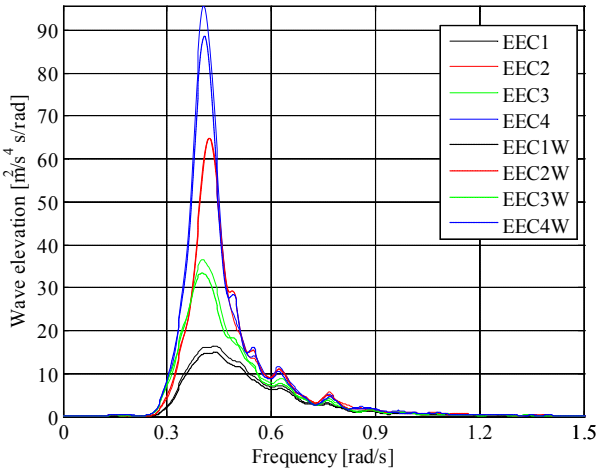

Figure 6. Comparison of spectra of wave elevation in WG2 for extreme environmental conditions

In Tables 7, 8 and 9 the statistical values of standard deviation, std, maximum, max, and mean values of the experimental data for surge, heave and pitch of semisubmersible platform and of WEC2 rotation for all the examined extreme conditions are presented. The statistical values are calculated by one hour time series of measured data (in full scale). As far as the std value, the effect of the wind loading is insignificant for the motions of the semisubmersible platform. The wind loading results to a small increase of the std value for the rotation of the WEC2. With regard to the maximum values of the motions, the wind loading results to the increase of the rotation of the WEC2 and to the increase of the surge motion of the platform especially for EEC2 and EEC4 conditions. As far as the mean values, the effect of the wind loading is presented mainly for EEC2W and EEC4W conditions and for surge and pitch motions of the semisubmersible platform. The largest max value that was measured experimentally is 15.095 m for surge motion, 5.53 m for heave motion, 4.911 deg for pitch motion and 24.380 deg for WEC2 rotation for EEC4W, EEC4, EEC4W and EEC4W conditions, respectively. It must be noted that the mean value of the thrust force (shear load at the top of tower) is equal to 24.19 kN, 34.36 kN, 201.4 kN and 30.56 kN for EEC1W, EEC2W, EEC3W and EEC4W, respectively.

Table 7. Standard deviation values of different motions for all extreme conditions

Motion	EEC1	EEC1W	EEC2	EEC2W
Surge (m)	1.520	1.525	2.510	2.485
Heave (m)	0.880	0.875	3.480	1.385
Pitch (deg)	0.4861	0.4834	0.7591	0.7122
WEC2 rot. (deg)	5.9793	6.1210	7.0961	7.0903
Motion	EEC3	EEC3W	EEC4	EEC4W
Surge (m)	2.175	2.195	3.010	3.050
Heave (m)	1.205	1.200	1.640	1.470
Pitch (deg)	0.6242	0.5869	0.8175	0.8412
WEC2 rot. (deg)	6.5329	6.7657	7.3163	7.7980

Table 8. Maximum values of different motions for extreme conditions

Motion	EEC1	EEC1W	EEC2	EEC2W
Surge (m)	6.295	6.260	12.090	12.670
Heave (m)	3.175	3.150	4.590	4.320
Pitch (deg)	2.3556	2.3786	3.2990	3.2136
WEC2 rot. (deg)	15.952	18.352	18.815	22.767
Motion	EEC3	EEC3W	EEC4	EEC4W
Surge (m)	11.210	10.765	13.970	15.095
Heave (m)	4.455	4.180	5.530	5.015
Pitch (deg)	2.8528	2.3340	3.9885	4.9114
WEC2 rot. (deg)	18.156	20.503	20.885	24.380

Table 9. Mean values of different motions for extreme conditions

Motion	EEC1	EEC1W	EEC2	EEC2W
Surge (m)	0.67	0.68	1.68	1.74
Heave (m)	0.06	0.09	0.05	0.04
Pitch (deg)	0.01	0.07	0.1	0.14
WEC2 rot. (deg)	0.0	0.0	0.0	0.0
Motion	EEC3	EEC3W	EEC4	EEC4W
Surge (m)	1.01	1.25	2.28	2.49
Heave (m)	0.25	0.04	0.15	0.13
Pitch (deg)	0.08	0.16	0.13	0.22
WEC2 rot. (deg)	0.0	0.0	0.0	0.0

In Figure 7 a comparison of the spectra of surge (Fig. 7i), heave (Fig. 7ii) and pitch (Fig. 7iii) of the semisubmersible platform for all the examined extreme conditions are presented. For the motions of the semisubmersible platform, the peaks of the spectra curves are observed close to the natural periods of each motion as calculated by the decay tests (Table 5); when a second peak is presented, it is observed close to the frequency of the excitation waves. For the surge motion an initial peak is presented close to ω=0.05 rad/sec dominated by the resonance of the platform; in this frequency range the wind loading has significant effect for the most of the examined conditions. For heave motion the peak of the spectra curves is observed close to the frequency of the excitation waves; the wind loading has as a result the decrease of the heave spectrum values close to that peak. For all of the examined motions the effect of the wind loading is intense for EEC4W. The effect of the wind loading on the spectra curves of the motions of the platform is insignificant for the mildest extreme environmental condition EEC1W.

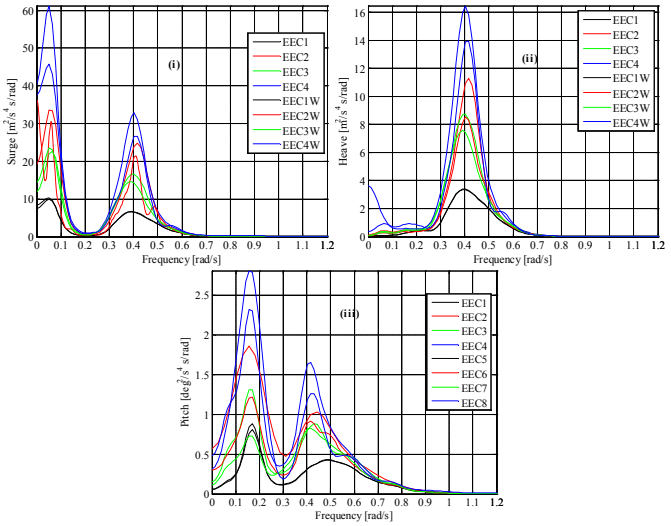

Figure 7. Comparison of spectra of surge (Fig. 7i), heave (Fig. 7ii) and pitch (Fig. 7iii) of semisubmersible platform

In Tables 10, 11 and 12 the one hour statistical standard deviation, std, maximum, max, and mean of the experimental data for different structural responses for all the examined extreme conditions are presented. These responses are the tension in the mooring line ML2, the bending moment at the tower's base, MX, the axial internal load in one arm of WEC2, FZ, and the torque in WEC2. As far as the std values, an increase of the std value of the tension of mooring line ML2 is observed as a result of the wind loading. The opposite is presented for the bending moment in the tower's base. For the internal loads associated with the WEC2 the effect of the wind loading is insignificant. With regard to the maximum values of the responses, the wind loading results to the small increase of the mooring line tension. The largest max value that was measured experimentally is 3,031.87 kN for mooring line ML2 tension, 5,196.88 kNm for tower's bending moment MX, 1,841.28 kNm for FZ internal load of one arm of WEC2 and 1307.12 kNm for torque of WEC2 for EEC4W, EEC4, EEC3W and EEC4W conditions, respectively. The wind loading does not affect the mean value of the structural responses significantly.

COMPARISONS OBTAINED WITH THE SFC FUNCTIONALITY MODEL

For the functionality model of SFC both regular and irregular wave tests without and with wind loadings have been conducted.

Table 10. Standard deviation values of different structural responses for extreme conditions

Structural response	EEC1	EEC1W	EEC2	EEC2W
ML2 tension (kN)	69.56	76.35	156.79	160.85
MX tower (kNm)	854.39	824.52	1,076.40	1,039.37
FZ WEC2 (kN)	105.59	103.15	124.76	124.27
Torque WEC2 (kNm)	133.77	139.25	138.92	140.63
Structural response	EEC3	EEC3W	EEC4	EEC4W
ML2 tension (kN)	119.80	124.29	106.05	126.52
MX tower (kNm)	966.25	879.62	1,050.64	978.56
FZ WEC2 (kN)	119.17	112.10	128.61	110.35
Torque WEC2 (kNm)	135.77	149.68	134.55	135.58

Table 11. Maximum values of different structural responses for extreme conditions

Structural response	EEC1	EEC1W	EEC2	EEC2W
ML2 tension (kN)	2,229.77	2295.58	2761.89	2790.03
MX tower (kNm)	3,317.79	3105.15	4826.81	4377.97
FZ WEC2 k(N)	1,722.41	1705.25	1746.00	1772.53
Torque WEC2 (kNm)	1,074.69	1058.58	1105.73	1050.58
Structural response	EEC3	EEC3W	EEC4	EEC4W
ML2 tension (kN)	2,561.80	2,586.85	2,965.27	3,031.87
MX tower (kNm)	3,962.37	3,503.71	5,196.88	5,186.36
FZ WEC2 (kN)	1,781.87	1,841.28	1,833.95	1,781.07
Torque WEC2 (kNm)	1,051.12	1,224.98	978.05	1,307.12

Table 12. Mean values of different structural responses for extreme conditions

Structural response	EEC1	EEC1W	EEC2	EEC2W
ML2 tension (kN)	1,765	1,765	1,785	1,794
MX tower (kNm)	0.0	0.0	0.0	0.0
FZ WEC2 (kN)	1,350	1,350	1,350	1,350
Torque WEC2 (kNm)	0.0	0.0	0.0	0.0
Structural response	EEC3	EEC3W	EEC4	EEC4W
ML2 tension (kN)	1,775	1,779	1,808	1,822
MX tower (kNm)	0.0	0.0	0.0	0.0
FZ WEC2 (kN)	1,350	1,350	1,350	1,350
Torque WEC2 (kNm)	0.0	0.0	0.0	0.0

Regular wave tests have been performed for a range of wave frequencies for estimating the RAOs of different response quantities of SFC. The regular wave tests have been performed without as well as with aligned wind loads. The waves propagate in the positive surge direction (+X). Regular waves with twelve different wave periods, Ti, i=1~12, were examined within the range 5.013 sec to 17.678 sec, while the examined wave height, H, was equal to 2 m (linear waves). During the regular waves with aligned wind loads the wind speed is equal to UWR=9.35 m/sec.

In Figure 8 the RAOs of surge, heave and pitch motions of the semisubmersible platform and rotation of WEC2 are presented. It is noted that the surge and heave motions of the platform are in m/m, the pitch is in deg/m and the rotation of WEC2 is in (degx0.1)/m units. For all the motions of the platform the effect of the wind loading on the amplitude of RAOs in general is small. The increase of the examined

period results to an increase of the RAOs for both surge and heave motion. It must be noted that for the case of regular waves with wind loading the mean value of the platform's surge (estimated by the time series of the motion) is larger 1.8 m compared to the mean value that the surge has for regular wave loading only. The amplitude of RAO as well as the mean value of the heave motion is not affected by the wind loading. The mean value of the amplitude of the pitch motion of the platform for the case of regular waves with wind loading is larger 2.2 deg compared to the mean value of the pitch amplitude for regular wave loading only. For the motions of the semisubmersible platform the effect of the wind loading as well as the effect of the aerodynamic damping is small attributed to the dominance of the inertial forces and potential damping. With regard to the rotation of WEC2, the wind loading results to the increase of the WEC2 rotation compared to the case that only wave loading exists. This is attributed to the larger mean pitch value of the platform that has as a result the WEC2 and WEC3 to be placed in higher positions in the vertical direction, closer to the MWL and applied to larger hydrodynamic loads. The resonance of the WEC2 rotation is observed for Ti=14.7 sec.

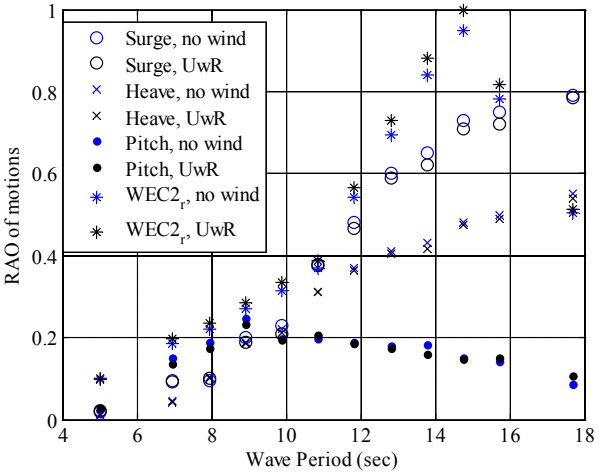

Figure 8. Comparison of RAO of surge, heave and pitch motions of semisubmersible platform and rotation of WEC2

The operational environmental conditions of the functionality model of SFC, for which comparisons of the wave-induced responses with wave-wind-induced responses based on experiments are conducted, are presented in Table 13. As far as the tests with wave and wind loading OEC1W ~ OEC3W the turbulence intensity of the measured wind data is 0.009. The mean value of the thrust force (shear load at the top of tower) is equal to 647.5 kN for the examined operational conditions.

Table 13. Examined operational environmental conditions in full scale values

Operational conditions	Hs (m)	Tp (sec)	Uw (m/sec)
OEC1	3.0	7.0	-
OEC2	3.0	9.0	-
OEC3	3.0	12.0	-
OEC1W	3.0	7.0	9.35
OEC2W	3.0	9.0	9.35
OEC3W	3.0	12.0	9.35

In Tables 14, 15 and 16 the one hour statistical std, max and mean of the experimental data for different responses for all the examined operational conditions are presented. These responses are the surge and pitch motions of the platform, the bending moment at the tower's base, MX, the axial internal load in one arm of WEC2, FZ, and the torque in WEC2. As far as the std values, an increase of the std value is observed mainly for MX tower and torque of WEC2 responses. With regard to the maximum values of the responses, the wind loading results to the significant increase of surge and pitch motions of the platform and of the MX tower bending moment. The wind loading affects the mean value of the surge and pitch motions of the platform.

Table 14. Standard deviation values of different structural responses for operational conditions

Response	OEC1	OEC1W	OEC2	OEC2W
Surge (m)	0.542	0.5914	0.373	0.397
Pitch (deg)	0.234	0.201	0.216	0.1825
MX tower (kNm)	674.83	1,286.48	571.62	1,242.39
FZ WEC2 (kN)	72.39	74.67	71.02	68.62
Torque WEC2 (kNm)	1,137.34	1,155.3	1,207.4	1,321.04
Response	OEC3	OEC3W		
Surge (m)	0.375	0.668		
Pitch (deg)	0.175	0.189		
MX tower (kNm)	384.8	1,198.5		
FZ WEC2 (kN)	54.93	53,382		
Torque WEC2 (kNm)	1,233.9	1,436.86		

Table 15. Maximum values of different structural responses for operational conditions

Response	OEC1	OEC1W	OEC2	OEC2W
Surge (m)	2.02	4.066	1.73	4.158
Pitch (deg)	0.85	2.983	1.033	3.007
MX tower (kNm)	3,199	4,682.3	2,308.1	4,310.5
FZ WEC2 (kN)	1,578.3	1,588	1,603.8	1,581.03
Torque WEC2 (kNm)	2,132.6	2,169.3	2,540.3	2,746.99
Response	OEC3	OEC3W		
Surge (m)	1.48	3.369		
Pitch (deg)	0.87	2.945		
MX tower (kNm)	1,566.5	3,582.9		
FZ WEC2 (kN)	1,550.2	1,553.1		
Torque WEC2 (kNm)	2,470.6	2,829.7		

Table 16. Mean values of different structural responses for operational conditions

Response	OEC1	OEC1W	OEC2	OEC2W
Surge (m)	0.86	2.59	0.76	2.848
Pitch (deg)	0.04	2.166	0.027	2.145
MX tower (kNm)	0.15	0.05	0.37	0.41
FZ WEC2 (kN)	1,350	1,350	1,350	1,350
Torque WEC2 (kNm)	0.27	0.33	0.51	0.29
Response	OEC3	OEC3W		
Surge (m)	0.552	2.39		
Pitch (deg)	0.023	2.141		
MX tower (kNm)	0.027	0.285		
FZ WEC2 (kN)	1,350	1,350		
Torque WEC2 (kNm)	0.225	1.22		

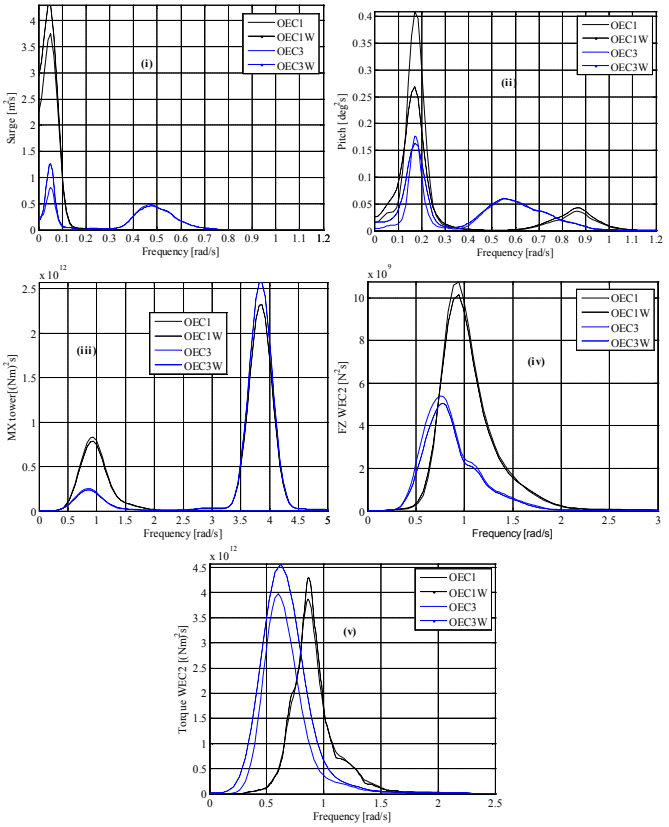

Figure 9. Comparison of spectra of surge (Fig. 9i), pitch (Fig. 9ii), bending moment at tower base (Fig. 9iii), FZ internal load of one arm of WEC2 (Fig. 9iv) and torque of WEC2 (Fig. 9v)

For the examined operational conditions the mean value of the surge and pitch motion for EC4, EC5 and EC6 is 1.8 m and 2.1 deg larger compared to EC1, EC2 and EC3, respectively, attributed to the wind loading. In Figure 9 spectral comparison of experimental responses of different parts of SFC are presented. As far as the motions of the platform, the resonance of each motion spectrum is presented for the frequency that corresponds to the motions natural frequency as calculated by the decay tests. The second peak (when it exists) in the motion curves is attributed to the examined wave frequency. The effect of the wind loading is significant for pitch motion while is smaller for surge motion. The effect of the wind loading is mainly presented for frequencies close to the natural frequencies of the motions of the platform. Regarding the bending moment in tower's base, MX, the resonance of the curve is presented for the first bending eigenfrequency of the tower of the wind turbine (ω=3.8 rad/sec) and only for operational environmental conditions with wind loading. As far as the structural responses of WEC2, for both responses, FZ and Torque, of WEC2 the resonance is observed close to the examined wave frequency. The effect of the wind loading is small for both structural responses.

As far as the functionality of the WECs of SFC, in Figure 10 bar plots of statistical quantities (mean, std and max) of the time series of the produced power of WEC2 are presented for OECi, i=1~6. An increase of the produced power is presented moving from OEC1 to OEC3 since the wave period is closer to the WECs' rotation natural period. The largest measured mean produced power is 70.2 kW for OEC6. On average 6%, an increase is presented for the conditions with wind loading compared to the conditions without wind loading, attributed to the larger obtained rotation of the WECs.

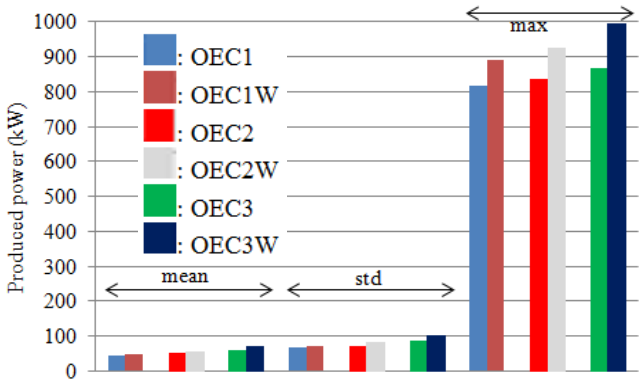

Figure 10. Comparison of statistical mean, std and max of the produced wave power of WEC2 for the examined operational conditions.

CONCLUSIONS

You should also comment that the model test only considers a constant and uniform wind field. If a turbulent wind field is considered, there will be more significant responses induced by wind.

In the present paper wave-induced responses are compared with wave-wind-induced responses based on experiments, of the combined wind/wave energy concept SFC. The comparison is conducted for two different experimental campaigns of SFC, namely the survivability and the functionality physical models of SFC, for extreme and operational environmental conditions respectively. The experiments of the SFC are conducted in an 1:50 scale physical model in the ocean basin at ECN.

For the survivability physical model of SFC, the effect of the wind loading is presented for the maximum values of the surge motion of the platform and of the rotation of the WEC2. The maximum absolute values of motions are presented for wave with wind loading conditions. The structural responses of mooring lines and wind turbines tower bending moment are affected by the wind loading, while, the structural responses related to WEC2 are insignificantly affected by the wind loading.

With regard to the functionality model and regular wave tests, the RAOs of the motions of the platform are not affected by the wind loading significantly. For the irregular wave tests the effect of the wind loading is large for pitch motion while is small for surge motion. Wind loading dominates the response of tower's bending moment. The effect of the wind loading in structural responses of different parts of WECs is small. A small increase of the produced power of the WECs is presented for conditions with wind loading.

The model tests were conducted with a constant and uniform wind field. If a turbulent wind field is accounted for more significant dynamic response induced by wind is expected.

ACKNOWLEDGEMENTS

The authors would like to acknowledge the financial support from the MARINA Platform project (Marine Renewable Integrated Application Platform, Grant Agreement no. 241402) under the European Community FP7 Energy Programme. The financial support for the construction of the physical model of SFC concept from the MARINA Platform is greatly acknowledged. Thomas Soulard and Sylvain Bourdier at ECN, France are highly appreciated for their work on the construction and execution of the tests of the physical SFC model. The financial support from the Research Council of Norway through the Centre for Ships and Ocean Structures and the Centre for Autonomous

Marine Operations and Systems, the Norwegian University of Science and Technology, is also acknowledged.

REFERENCES

Azcona, J, Bouchotrouch, F, González, M, Garciandía, J, Munduate, X, Kelberlau, F, and Nygaard, T.A (2014). "Aerodynamic Thrust Modelling in Wave Tank Tests of Offshore Floating Wind Turbines Using a Ducted Fan," *Journal of Physics: Conf. Series,* 524, 012089.

Courbois, A (2013). "Etude expérimentale du comportement dynamique d'une éolienne offshore flottante soumise à l'action conjuguée de la houle et du vent," Ph.D. thesis, Ecole Centrale de Nantes (in French).

Flocard, F, and Finnigan, T.D. (2010). "Laboratory experiments on the power capture of pitching vertical cylinders in waves," *Ocean Engineering*, 37, 989-997.

Fowler, M.J., Kimball, R.W., Thomas, D.A., and Goupee, A.J (2013). "Design and Testing of Scale Model Wind Turbines for Use in Wind/Wave Basin Model Tests of Floating Offshore Wind Turbines," *Proceedings of the ASME 2013 32nd International Conference on Ocean, Offshore and Arctic Engineering*, OMAE2013-10122, June 9-14, Nantes, France.

Gao, Z, Moan, T, Wan, L, and Michailides, C (2015). "Comparative numerical and experimental study of two combined wind and wave energy concepts," *Journal of Ocean Engineering and Science*, (Accepted for publication).

H2Ocean (online). Available at: http://www.h2ocean-project.eu/ [Accessed in December 2015].

Huijs, F, Ridder, E.J., and Savenije, F (2014). "Comparison of model tests and coupled simulations for a semi-submersible floating wind turbine," *Proc of the 33rd Int Conf on Oc, Off and Arc Eng.*. OMAE2014-23217, San Francisco, USA

Jonkman, J, Butterfield, S, Musial, W, and Scott, G (2009). "Definition of a 5-MW Reference Wind Turbine for Offshore System Development," *National Renewable Energy Laboratory*, Technical Report, NREL/TP-500-38060, Boulder.

Jonkman, J.M., and Matha, D (2011). "Dynamics of offshore floating wind turbines-analysis of three concepts," *Wind Energy*, 14(4), 557–569.

Karimirad, M, and Michailides, C (2015). "V-shaped semisubmersible offshore wind turbine: An alternative concept for offshore wind technology," *Renewable Energy*, 83, 126-143.

Li, L, Gao, Z, and Moan, T (2015). "Joint Distribution of Environmental Condition at Five European Offshore Sites for Design of Combined Wind and Wave Energy Devices," *Journal of Offshore Mechanics and Arctic Engineering*, 137, 031901-1.

Luan, C, Michailides, C, Gao Z, Moan T (2014). "Modeling and analysis of a 5 MW semi-submersible wind turbine combined with three flap-type Wave Energy Converters," *Proc of the 33rd International Conference on Ocean, Offshore and Arctic Engineering*, no.OMAE2014-24215, pp. V09BT09A028, doi:10.1115/OMAE2014-24215.

Luan, C, Gao, Z, and Moan, T (2015). "Conceptual designs of a 5-MW and a 10-MW semi-submersible wind turbine with emphasis on the design procedure," (Under review).

World Energy Council (2013). "World Energy Perspective: Cost of Energy Technologies", ISBN: 978 0 94612 130 4.

MARINA Platform (Online). Available at: http://www.marina-platform.info/index.aspx [Accessed in December 2015].

Martin, H.R., Kimball, R.W., Viselli, A.M., and Goupee, A.J (2012). "Methodology for Wind/Wave Basin Testing of Floating Offshore Wind Turbines," *Proceedings of the ASME 2012 31st International Conference on Ocean, Offshore and Arctic Engineering*, OMAE2012-83627, July 1-6, Rio de Janeiro, Brazil.

MERMAID (Online). Available at: http://www.mermaidproject.eu/ [Accessed in October 2015].

Michailides, C (2015). "Power Production of the Novel WLC Wave Energy Converter in Deep and Intermediate Water Depths," *Recent Patents on Engineering*, 9, 42-51.

Michailides, C, Luan, C, Gao, Z, and Moan, T (2014). "Effect of Flap Type Wave Energy Converters on the Response of a Semi-submersible Wind Turbine in Operational Conditions," *Proc of the 33rd International Conference on Ocean, Offshore and Arctic Engineering*. OMAE2014-24065, pp V09BT09A014, doi:10.1115/OMAE2014-24065.

Michailides, C, Gao, Z, and Moan, T (2015). "Response Analysis of the Combined Wind/Wave Energy Concept SFC in Harsh Environmental Conditions," *Renewable Energies Offshore - 1st International Conference on Renewable Energies Offshore, RENEW 2014*, pp. 877-884.

Michailides, C, Gao, Z, and Moan, T (2016a). "Experimental and numerical study of the response of the offshore combined wind/wave energy concept SFC in extreme environmental conditions," (Under review).

Michailides, C, Gao, Z, and Moan, T (2016b). "Experimental Study of the Functionality of a Semisubmersible Wind Turbine Combined with Flap-Type Wave Energy Converters," (Under review).

Muliawan, M.J., Karimirad, M, and Moan, T (2013). "Dynamic response and power performance of a combined spar-type floating wind turbine and coaxial floating wave energy converter," *Renewable Energy*, 50, 47–57.

Müller, K, Sandner, F, Bredmose, H, Azcona, J, Manjock, A, and Pereira, R (2014). "Improve Tank Test Procedures for Scaled Floating Offshore Wind Turbines," *The International Wind Engineering Conference – Support Structures & Electrical Systems*. September 3-4, Hannover, Germany.

Ogai, S, Umeda, S, and Ishida, H (2010). "An experimental study of compressed air generation using a pendulum wave energy converter," *Journal of Hydrodynamics*, 22(5), 290-295.

Olav Olsen AS (Online). Available at: http://www.olavolsen.no/node/82 [Accessed 10 December 2015].

ORECCA (Online). Available at: http://www.orecca.eu/ [Accessed in December 2015].

Pecher, A, Kofoed, J.P., Espedal, J, and Hagberg, S (2010). "Results of an experimental study of the langlee wave energy converter," *20th International Offshore and Polar Engineering Conference*, ISOPE, Beijing; China.

O'Sullivan, K, and Murphy, J (2013). "Techno-Economic Optimisation of an Oscillating Water Column Array Wave Energy Converter," *Proc. of the 10th European Wave and Tidal Energy Conference*, Aalborg, Denmark.

Robertson, A, Jonkman, J, Masciola, M, Song, H, Goupee, A, Coulling, A, and Luan, C (2014). "Definition of the Semisubmersible Floating System for Phase II of OC4,", *National Renewable Energy Laboratory,* Golden, CO, U.S.A, 2014, NREL/TP-5000-60601.

Roddier, D, Cermelli, C, Aubault, A, and Weinstein A (2010). "WindFloat: A floating foundation for offshore wind turbines," *Journal of Renewable and Sustainable Energy,* 2(3), 033104-1-033104-34.

TROPOS (Online). Available at: http://www.troposplatform.eu/ [Accessed in December 2015].

Wan, L, Gao, Z, Moan, T (2015). "Coastal Engineering, Experimental and Numerical Study of the Hydrodynamic Responses of a Combined Wind and Wave Energy Converter Concept in Survival Modes," *Coastal Engineering*, 104, 151–169.

Wan, L, Gao, Z, Moan, T, and Lugni, C (2016). "Comparative experimental study of the survivability of a combined wind and wave energy converter in two testing facilities," *Ocean Engineering*, 111, 82–94.